

Nanoparticulate magnetite thin films as electrode materials for the fabrication of electrochemical capacitors

Suh Cem Pang · Wai Hwa Khoh · Suk Fun Chin

Received: 10 December 2009 / Accepted: 14 May 2010 / Published online: 25 May 2010
© Springer Science+Business Media, LLC 2010

Abstract Magnetite nanoparticles in stable colloidal suspension were prepared by the co-precipitation method. Nanoparticulate magnetite thin films on supporting stainless steel plates were prepared by drop-coating followed by heat treatment under controlled conditions. The effects of calcination temperature and atmosphere on the microstructure and electrochemical properties of nanoparticulate magnetite thin films were investigated. Nanoparticulate magnetite thin films prepared under optimized conditions exhibited a specific capacitance value of 82 F/g in mild aqueous 1.0 M Na₂SO₄ solution. Due to their high charge capacity, good cycling reversibility, and stability in a mild aqueous electrolyte, nanoparticulate magnetite thin films appear to be promising electrode materials for the fabrication of electrochemical capacitors.

Introduction

The ever increasing miniaturization of portable electronic and communication devices such as laptop, cellular phones, and personal digital assistants (PDA) have led to increasing demands for energy-storage systems with high power capability and energy density, high reversibility, and long cycle life. Due to the low power capability of batteries and the low energy density of conventional capacitors, these charge storage systems are unable to meet the demands of modern devices, which require both high

power capability and high energy density. Electrochemical capacitors which possess high power capability and moderately high energy density are able to fill in the gap between batteries and conventional capacitors. In addition, the energy-storage mechanisms in electrochemical capacitors are simpler and highly reversible which ensure a very long cycle life of exceeding 100,000 cycles [1, 2].

Recently, various types of transition metal oxides such as manganese oxides and ruthenium oxides have been investigated as electrode materials for the fabrication of electrochemical capacitors. Each of these materials possesses its own limitations and advantages [3, 4]. Nanoparticulate magnetite (Fe₃O₄) thin film is another potential electrode material which has received considerable attention due to its superior electrochemical properties, environmental friendliness, and low cost. Wu et al. reported that magnetite crystallites electrocoagulated on conductive matrix exhibited specific capacitance values that varied over a large range between 30 and 500 F/g in 1.0 M Na₂SO₃ aqueous electrolytes [5, 6]. However, studies by Wu et al. focused only on the electrochemical properties of magnetite nanocrystallites without considering the effects of surface morphology and microstructure on their electrochemical properties. Elucidating the microstructure–property relationship for the magnetite electrodes is crucial for enhancing their electrochemical properties by optimizing their surface morphological characteristics and microstructural parameters. In this study, we have focused on the characterization of nanoparticulate magnetite thin films prepared under various synthesis and post-synthesis conditions, and elucidating the effects of microstructure on their electrochemical properties. Besides, the potential utility of nanoparticulate magnetite thin films as electrode materials for the fabrication of electrochemical capacitors was evaluated.

S. C. Pang (✉) · W. H. Khoh · S. F. Chin
Faculty of Resource Science and Technology, Department
of Chemistry, Universiti Malaysia Sarawak, 94300 Kota
Samarahan, Sarawak, Malaysia
e-mail: scpang@frst.unimas.my; suhcem@gmail.com

Experimental

Preparation of magnetite colloidal suspension

Magnetite colloidal suspension was prepared based on the co-precipitation method as reported in the literature [7, 8]. The stoichiometric solution mixture of 1 mol of Fe^{2+} and 2 mol of Fe^{3+} was added slowly to an excess ammonia solution, which was vigorously stirred and maintained at a temperature of 80 °C. Great care was taken to exclude oxygen during all stages of the preparation by continuously de-aerating all solutions with purified nitrogen. Magnetite was formed based on the chemical Eq. 1



The magnetite precipitate formed was separated by magnetic settling, and washed three times with deaerated ultrapure water. The purified magnetite precipitate was then redispersed in 100 mL ultrapure water, and the resulting magnetite colloidal suspension was maintained at a pH above 9 for enhanced stability [9, 10].

Preparation of magnetite thin films and xerogels

Nanoparticulate magnetite thin films were prepared on precleaned stainless steel plates by the drop-coating technique. The relative film thickness was controlled by the magnetite loadings (30 μmol or 120 μmol) which was associated with a fixed volume of magnetite colloidal suspension (0.1–0.4 mL) that covered a known area ($1.5 \text{ cm} \times 1.5 \text{ cm}$) of the stainless steel plate. A small amount of methylcellulose ($\sim 7.0 \times 10^{-2}$ wt%) was being added to increase the viscosity of the colloidal suspension in order to improve adherence and prevent cracking of magnetite films formed on the stainless steel plates. The magnetite loading of thin films prepared was determined quantitatively by atomic absorption spectroscopy (AAS).

Xerogels of magnetite were prepared by evaporating a given volume of magnetite colloidal suspension in a desiccator filled with anhydrous silica gels. Magnetite xerogels formed were subsequently calcined in a tube furnace at temperatures up to 500 °C in nitrogen atmosphere for 1 h.

Characterization of magnetite thin films and xerogels

The surface morphology of magnetite thin films was observed using a field emission scanning electron microscope (FESEM, LEO 1525). The specific surface area and pore size distribution of magnetite xerogels calcined at various temperatures were determined by the BET nitrogen adsorption/desorption method (Micromeritics ASAP 2010). The electrochemical properties of magnetite thin films were characterized by cyclic voltammetry (CV) using a

standard three-electrode cell configuration. A saturated calomel electrode (SCE) fitted with a Vycor bridge, and a platinum foil ($\sim 2 \text{ cm}^2$) were used as the reference electrode and the counter electrode, respectively. In all cyclic voltammetric experiments, a geometric area of 0.1257 cm^2 of each thin film sample was being exposed to 1.0 M Na_2SO_4 aqueous electrolyte. Cyclic voltammograms (CV) were generated by scanning within the potential range of 0.0–1.0 V (vs. SCE) at a scan rate of 50 mV/s.

Results and discussion

Figure 1 shows the FESEM micrographs of magnetite thin films on stainless steel plates and calcined at various temperatures in nitrogen atmosphere for 1 h. The EDX spectra of magnetite thin films (Fig. 1a–c) showed that these films consisted primarily of Fe and O elements, thereby confirming the presence of magnetite. These films were observed to be nanoparticulate and porous in nature with particle sizes ranged from 5 nm to 31 nm. The porous nature of these films could be attributed to the formation of particle agglomerates upon evaporation of the solvent. The calcination temperature was observed to have substantial effect on the microstructure of magnetite films. As the calcination temperature was increased, the surface morphology of magnetite thin films became rougher and denser. The calcination process should result in the removal of structural water and residual solvent molecules, thereby led to increased density of magnetite films. The mean particle size of magnetite increased with calcination temperature from 10 nm at 100 °C, 12 nm at 300 °C, to 16 nm at 500 °C, which could be attributed to the microstructure evolution of magnetite thin films upon calcination through stages such as dehydroxylation, crystallization, and grain coarsening [11].

Figure 2 shows the effect of calcination temperature on the specific surface area and total pore volume of magnetite xerogels. Both the specific surface area and total pore volume were observed to increase at calcination temperature of 100 °C, but decreased substantially at higher calcination temperatures of 300 and 500 °C. The increase in the specific surface area at 100 °C could be attributed to the removal of physisorbed water and solvent molecules retained within the films which led to the formation of pores within the oxide matrices. Besides, densification of xerogel samples due to the collapse of micro- and mesopores, as well as particle growth, had resulted in decreased specific surface area at higher calcination temperature.

Figure 3 shows the effect of calcination temperature on the specific surface area and adsorption pore size distribution of magnetite xerogels. In general, the pore size

Fig. 1 SEM micrographs and EDX spectra of nanoparticulate magnetite thin films calcined in nitrogen atmosphere for 1 h at: **a** 100 °C, **b** 300 °C, and **c** 500 °C

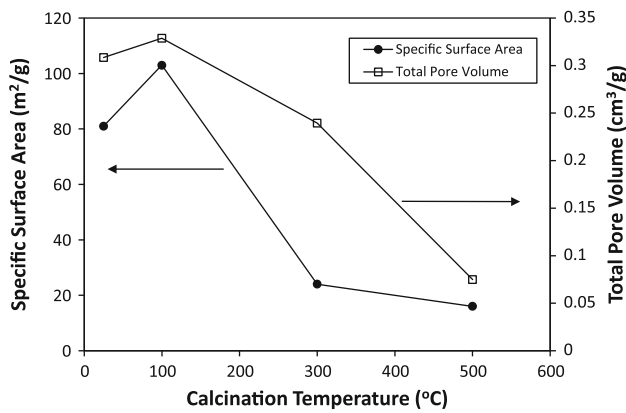
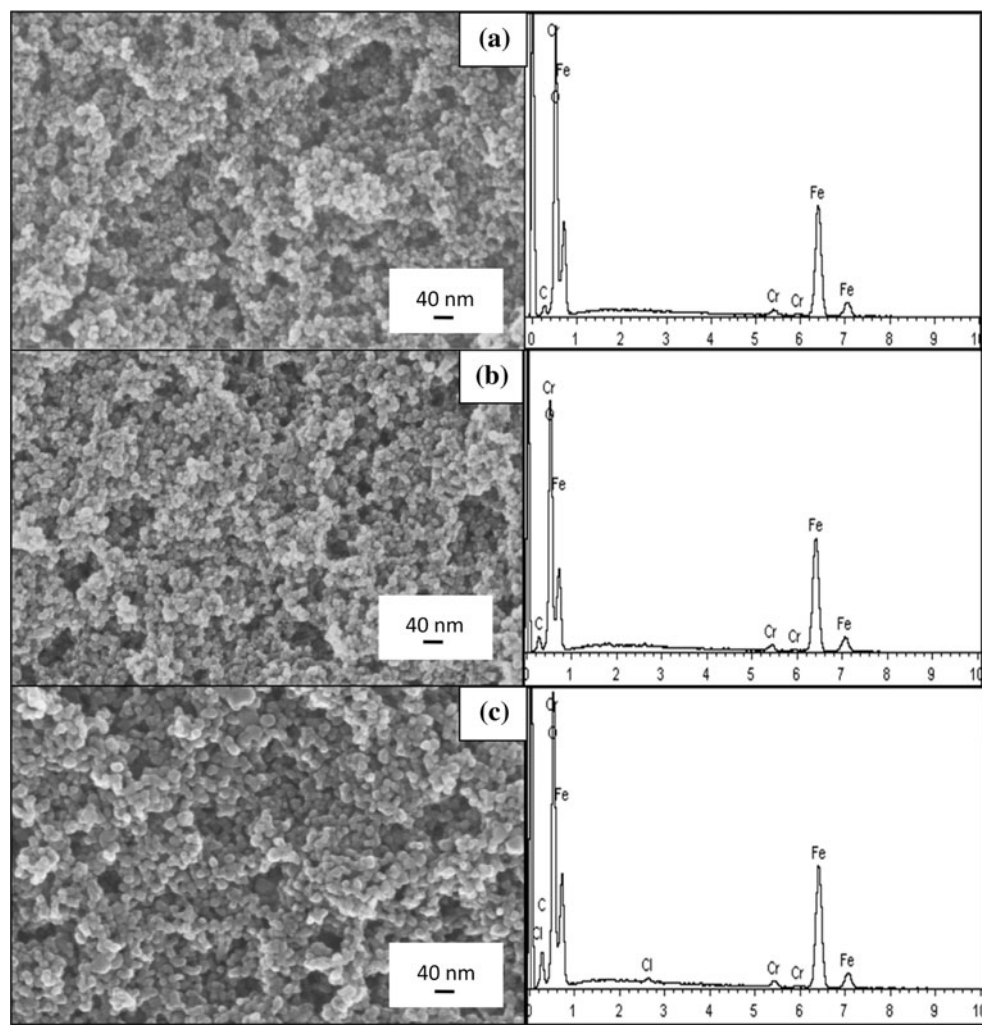


Fig. 2 Effect of calcination temperature on the specific surface area and total pore volume of magnetite xerogels

distributions of magnetite xerogels were observed to shift gradually towards larger pore diameters, and with substantial reduction in the total cumulative pore volume for xerogel sample calcined at higher temperatures (>100 °C). This could be attributed to increased densification of

xerogels at higher calcination temperatures. Magnetite xerogels calcined at 100 °C possessed the highest specific surface area as compared to xerogels as prepared at room temperature, and xerogels calcined at 300 and 500 °C. For xerogels calcined at 100 °C, 65% of total pore volume was attributed to macropores, whereas 24% and 11% of total pore volume were attributed to meso- and micropores, respectively. In contrast, for xerogels that had been calcined at 300 °C, the total pore volume contributed by macropores had increased substantially, whereas total pore volume contributed by both meso- and micropores had decreased substantially. Henceforth, the substantially lower specific surface areas of magnetite xerogels calcined at 300 and 500 °C were attributed to densification resulting from the collapse of both meso- and micropores.

Figure 4 shows the CV of nanoparticulate magnetite thin films that had been calcined in either nitrogen or air at 300 °C for 1 h. The CV curve of the magnetite thin film calcined in air was observed to be very narrow as compared to that of film calcined in nitrogen. The charge capacities of magnetite thin films that had been calcined in nitrogen and

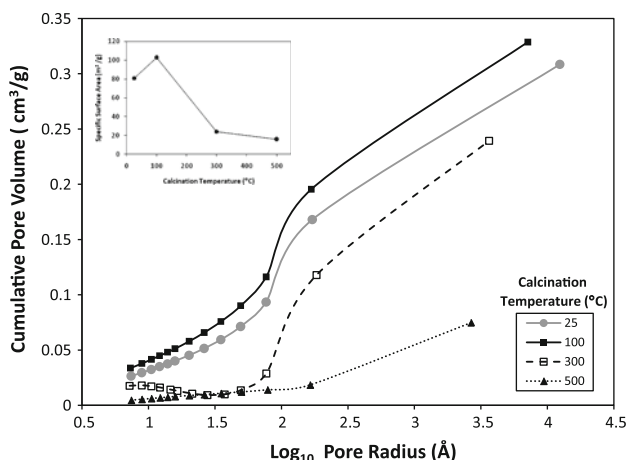


Fig. 3 Effect of calcination temperature on the adsorption pore size distribution of magnetite xerogels. Inset shows the specific surface areas (SSA) of magnetite xerogels calcined at various temperatures

air were calculated to be 186 and 49 mF/cm², respectively. In the presence of oxygen, magnetite oxidizes slowly to maghemite ($\gamma\text{-Fe}_2\text{O}_3$) at room temperature, and then to hematite ($\alpha\text{-Fe}_2\text{O}_3$) at higher temperatures [12]. Besides, magnetite particles prepared in aqueous medium would be transformed into maghemite at about 200 °C, and oxidation could occur spontaneously at room temperature to form iron oxide with a unit cell parameter (8.36 Å) in between that of magnetite (8.40 Å) and maghemite (8.33 Å) [13]. Maghemite and hematite are less conductive electrically than magnetite due to their very low Fe²⁺ state donor density [14]. In edge sharing octahedral of magnetite, the Fe²⁺ and Fe³⁺ ions on the octahedral sites are close together such that the holes can migrate easily from Fe²⁺ to Fe³⁺. With a conductivity of 102–103 Ω⁻¹ cm⁻¹, magnetite has the lowest resistivity as compared to maghemite (n type semiconductor with band gap 2.03 eV) and hematite (n type semiconductor with band gap 2.2 eV). On the other hand, magnetite is both an n- and p-type semiconductor

with the smallest band gap of 0.1 eV. Magnetite thin films that had been calcined in air were no longer pure magnetite but a mixture of magnetite, maghemite, and hematite, and hence the lower charge capacity observed.

Nanoparticulate magnetite thin films with different relative thickness in terms of different magnetite loading of 0.4–1.6 μmol/cm² were prepared by the drop-coating technique. The relative film thicknesses were controlled by the volume of the colloidal suspension used per unit area of thin film formed. A small amount of methylcellulose (about 7.0×10^{-2} wt%) was added to increase the viscosity of the magnetite colloidal suspension, which in turn enhanced the coating process with improved film adherence to the supporting substrate. Figure 5a shows the CV of magnetite thin films with different relative film thickness over the potential range of 0.0–1.0 V (vs. SCE). The almost rectangular shape of all CV curves indicated good capacitive behavior of magnetite thin films. Figure 5b shows the effect of relative film thickness on the charge capacity and specific capacitance of magnetite thin films calcined at 300 °C in nitrogen. The charge capacities of magnetite films were observed to increase with increasing relative film thickness. Thicker magnetite films were associated with higher loadings of electroactive material and hence the higher charge capacities observed. The charge capacities of magnetite films with magnetite loadings of 0.4 and 1.6 μmol/cm² were 60 mF/cm² (or 82 F/g) and 103 mF/cm² (or 35 F/g), respectively. However, the rate of increase in charge capacity was observed to decline gradually for films of higher magnetite loadings, which could be attributed to the combined effect of higher resistivity of thicker films, and reduced accessibility of electrolyte ions to active sites within the bulk phase of thicker films. Despite higher magnetite loadings, the inherent lower material utilization efficiency of thicker films led to decrease in their specific capacitances.

The charge capacities of nanoparticulate magnetite thin films were observed to be strongly affected by the calcination temperature. Figure 6a shows the CV of magnetite thin films that have been calcined at different temperatures between 100 and 500 °C in nitrogen for 1 h. The charge capacities of magnetite films were determined from the areas of CV curves as a function of the calcination temperature (Fig. 6b). The charge capacities of magnetite thin films of fixed magnetite loading increased with increasing calcination temperature up to 300 °C, but decreased substantially at calcination temperatures above 300 °C. A maximum charge capacity of 68 mF/cm² was achieved for magnetite thin films calcined at 300 °C. Charge capacities of films calcined at 100 and 500 °C were substantially lower at 19 and 41 mF/cm², respectively. Films without any heat treatment were observed to possess a charge capacity of about 13 mF/cm² only.

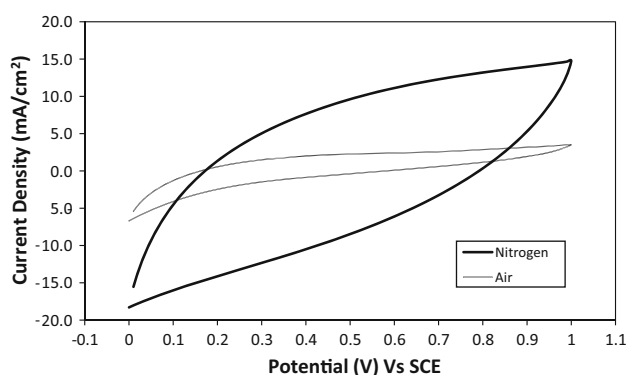


Fig. 4 Cyclic voltammograms (CV) of nanoparticulate magnetite thin films after being heat treated under different atmospheres

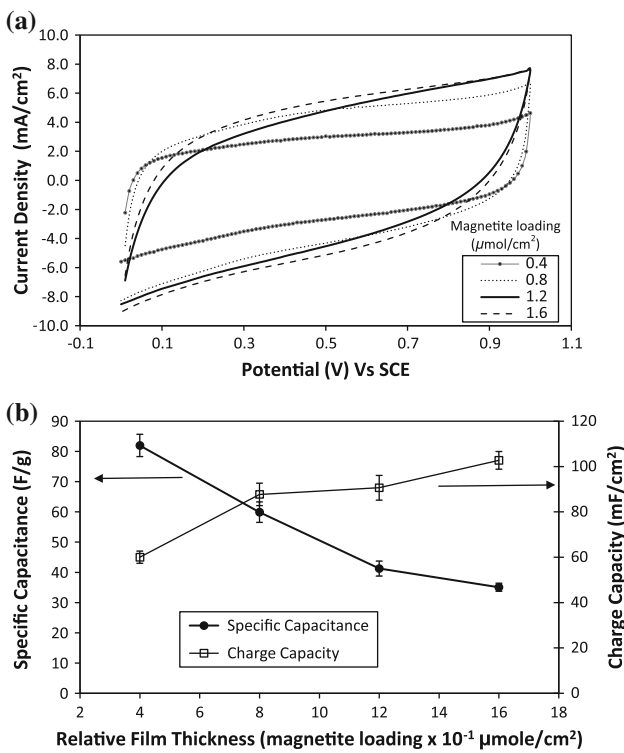


Fig. 5 Effect of relative film thickness or magnetite loading on the **a** shape of CV curves, and **b** capacitive behaviors of nanoparticulate magnetite thin films

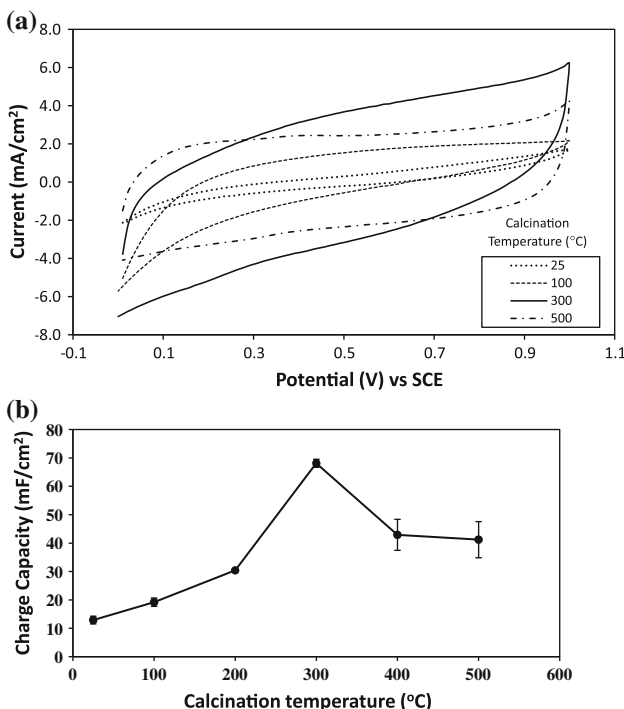


Fig. 6 Effect of calcination temperature on the **a** size and shape of CV curves, and **b** charge capacities of nanoparticulate magnetite thin films

Theoretically, the charge capacities of nanoparticulate magnetite thin films should correlate positively to their specific surface areas since high surface areas should enhance accessibility of electrolyte ions to active sites of electrode materials. However, the charge capacity and capacitive behavior of magnetite thin films were greatly influenced by their microstructural parameters such as mean pore size and pore size distribution. Since the size of hydrated ions in an aqueous electrolyte is within the range of 6–7.6 Å, the minimum effective pore size should be greater than 15 Å. In general, a pore size within the range of 30–50 Å is required to maximize the capacitance of an electric double-layer capacitor [15]. In this study, substantially higher charge capacity was obtained from magnetite thin film calcined at temperature 300 °C with the highest mean pore radius of 14.5 Å as compared with those of films without heat treatment (6.5 Å), calcined at 100 °C (6.5 Å) or 500 °C (5.7 Å). The higher charge capacity of films calcined at 300 °C could be due to their considerably larger mean pore radius, which in turn, enabled electrolyte ions to penetrate deeply into active sites within the bulk of oxide matrices, and hence led to enhanced utilization of active materials.

Figure 7 shows CV of the same magnetite thin film in three different aqueous electrolytes of the same cationic but different anionic electrolyte species. Wang et al. reported that the capacitive behavior of magnetite films were very sensitive to the anionic electrolyte species but not the alkaline metal cations. As shown in Fig. 7, the magnetite film was observed to exhibit distinctively different capacitive behaviors in different aqueous electrolytes within the same potential scan window (0.0 to +1.0 V vs. SCE). Presumably, such different capacitive behavior was attributed mainly to the different pH values of these aqueous electrolytes. Indeed, these aqueous electrolytes (at 1.0 M) showed different pH values at room temperature: Na₂SO₄ (pH ~7); Na₂SO₃ (pH ~9); and Na₃PO₄ (pH ~12). As such, magnetite thin films would exhibit reversible capacitive behavior over different applicable potential ranges where major faradaic redox reactions could take place.

Wu et al. reported that the specific capacitances of mixed electrode containing magnetite:carbon black in the ratio of 9:1 were 27.0, 5.3, and 7.6 F/g-Fe₃O₄ in 1 M aqueous electrolytes of Na₂SO₃ and Na₂SO₄, and in saturated Na₃PO₄, respectively, over the scan potential window of -1.2 V to +1.0 V vs. Ag/AgCl. However, the charge capacities of magnetite electrodes in Na₂SO₃ aqueous electrolyte were greatly affected by the dispersed magnetite crystallites on the conductive matrix, with their specific capacitances varied substantially between ~30 F/g and 510 F/g. Such different capacitive behaviors were attributed to the limited conductivity of pure magnetite which

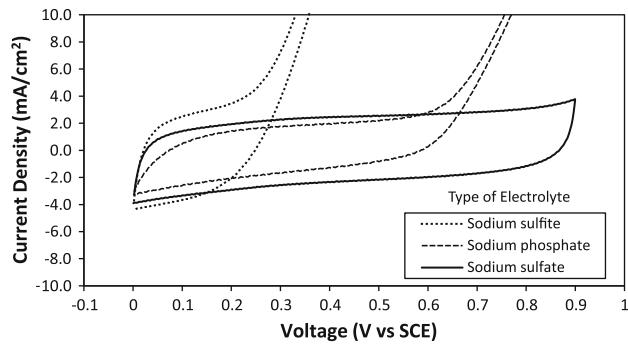


Fig. 7 Effect of electrolyte composition on the capacitive behavior of nanoparticulate magnetite thin film

could be enhanced by adding optimum amount of conductive additive such as carbon black to form composite or mixed electrode. Indeed, pure magnetite electrode was reported to exhibit a specific capacitance of less than 0.1 F/g- Fe_3O_4 in 1 M Na_2SO_3 , but it increased to about 30 F/g- Fe_3O_4 with an addition of 10 wt% of carbon black. The specific capacitance of coprecipitated electrode of 3 wt% of magnetite loading was reported to be as high as ~ 510 F/g- Fe_3O_4 in 1 M Na_2SO_3 aqueous electrolyte [5, 6].

In contrast to the preceding findings by Wu et al. and Wang et al., the specific capacitances of nanoparticulate magnetite thin films ($\sim 100\%$ pure magnetite) prepared under various synthesis conditions in this study were observed to vary between 35 and 82 F/g- Fe_3O_4 in 1.0 M sodium sulfate aqueous electrolyte. The highest specific capacitance of 82 F/g- Fe_3O_4 in 1.0 M sodium sulfate was obtained for optimized magnetite thin film of magnetite loading of $0.4 \mu\text{mol}/\text{cm}^2$ and heat treated at 300 °C in nitrogen. These specific capacitance values of pure nanoparticulate magnetite thin films in sodium sulfate aqueous electrolyte were substantially higher than those of pure magnetite and magnetite/carbon black (9:1) composite electrodes in various aqueous electrolytes including sodium sulfite as previously reported. These observed different capacitive behaviors could be mainly attributed to microstructural effects (as shown in Figs. 2, 3) associated with the nanoparticulate and highly porous nature of magnetite thin films prepared in the present study.

Figure 8 shows the effect of long-term cycling of nanoparticulate magnetite thin films that had been calcined at 300 °C in 1.0 M Na_2SO_4 aqueous electrolyte. The charge capacities of magnetite films were observed to decrease rapidly for the initial 100 cycles, but thereafter decreased very gradually over the span of 1,000 cycles. Chemical degradation and transformation of magnetite in aqueous electrolyte to other forms of iron oxides such as maghemite and hematite in the presence of oxygen could have resulted in the observed decline in charge capacities

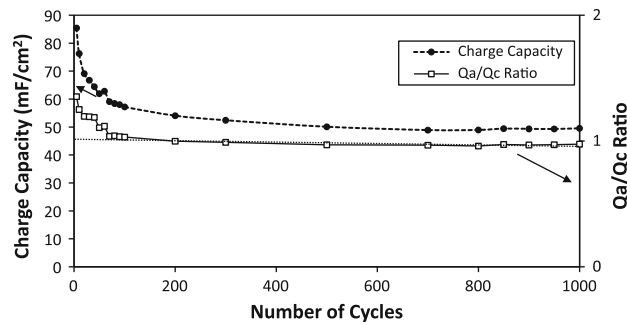


Fig. 8 Effect of long-term cycling on the charge capacity of magnetite nanoparticulate thin films

of magnetite thin films during long-term cycling [16]. Furthermore, the oxygen evolution reaction could affect the electrode/current collector interface, and exacerbated corrosion of the current collector would lead to higher equivalent series resistance (ESR) of the electrode [17]. The anodic/cathodic charge ratios (Q_a/Q_c) for the initial 100 cycles were larger than one, but thereafter have remained virtually one over the span of 1,000 cycles. This indicated that magnetite thin film exhibited high cycling reversibility except for the initial 100 cycles or so, which could be attributed to incomplete penetration of electrolyte ions into the bulk of electroactive material.

Conclusion

Our study has demonstrated that the calcination temperature could have substantial effect on the overall microstructure and charge capacities of nanoparticulate magnetite thin films. Enhanced electrochemical properties were observed for magnetite thin films that had been calcined at 300 °C in nitrogen, which could be attributed to optimized microstructure of films, and consequently, enhanced accessibility of electrolyte ions to electroactive sites within the oxide matrices. Given their ease of preparation, low cost, and low toxicity, nanoparticulate magnetite thin films appeared to be a promising electrode material for the fabrication of electrochemical capacitors. Further optimization and enhancement of electrochemical properties is envisaged through better microstructural control of these nanoparticulate magnetite thin films.

Acknowledgement This work was funded by Malaysian Ministry of Science Technology and Innovation (MOSTI) through the IRPA Grant No. 03-02-09-1019 EA001.

References

- Pang SC, Anderson MA, Chapman TW (2000) J Electrochim Soc 147(2):444

2. Chin SF, Pang SC, Anderson MA (2002) *J Electrochem Soc* 149(4):A379
3. Pang SC, Anderson MA (2000) *J Mater Res* 15:2096
4. Jang JH, Han S, Hyeon T, Oh SM (2003) *J Power Sources* 123:79
5. Wu NL, Wang SY, Han CY, Wu DS, Shiue LR (2003) *J Power Sources* 113:173
6. Wang SL, Wu NL (2003) *J Appl Electrochem* 33:345
7. Massart R (1981) *IEEE Trans Magn MAG-17:1247*
8. Chin SF, Iyer KS, Raston CL, Saunders M (2008) *Adv Funct Mater* 18:922
9. Pang SC, Chin SF, Anderson MA (2007) *J Colloid Interface Sci* 311:94
10. Chin SF, Makha M, Raston CL and Saunders M (2007) *Chem Commun* 1948
11. Wu NL (2002) *Mater Chem Phys* 75:6
12. Cornell RM, Schwertmann U (2003) *The iron oxides: structure, properties, reactions, occurrences and uses*, 2nd edn. Wiley-VCH, Germany
13. Wieland J, Goossens V, Hausbrand R, Terryn H (2007) *Electrochim Acta* 52:7617
14. Jolivet JP, Tronc E (1987) *J Colloid Interface Sci* 125:688
15. Conway BE (1991) *Electrochemical supercapacitors scientific fundamentals and technological applications*. Kluwer Academic/Plenum Publishers, New York
16. Castro PA, Vago ER, Calvo EJ (1996) *J Chem Soc Faraday Trans* 92:3371
17. Elanger D, Brousse T, Jeffrey WL (2008) *Electrochim Soc Interface* 49